Aqueous Uranium(VI) Concentrations Controlled by Calcium Uranyl Vanadate Precipitates[1]

Tetsu K. Tokunaga,* Yongman Kim, Jiamin Wan, and Li Yang

Earth Sciences Division, Lawrence Berkeley National Laboratory, Berkeley, California 94720, United States

Supporting Information

ABSTRACT: Elevated concentrations of U in contaminated environments necessitate understanding controls on its solubility in groundwaters. Here, calculations were performed to compare U(VI) concentrations expected in typical oxidizing groundwaters in equilibrium with different U(VI) minerals. Among common U(VI) minerals, only tyuyamunite ($Ca(UO_2)_2V_2O_8{\cdot}8H_2O$), uranophane ($Ca(UO_2)_2(SiO_3OH)_2{\cdot}5H_2O$), and a putative well-crystallized becquerelite ($Ca(UO_2)_6O_4(OH)_6{\cdot}8H_2O$) were predicted to control U concentrations around its maximum contaminant level (MCL = 0.13 μM), albeit over narrow ranges of pH. Given the limited information available on uranyl vanadates, room temperature Ca−U−V precipitation experiments were conducted in order to compare aqueous U concentrations with tyuyamunite equilibrium predictions. Measured U concentrations were in approximate agreement with predictions based on Langmuir's estimated ΔG_f°, although the precipitated solids were amorphous and had wide ranges of Ca/U/V molar ratios. Nevertheless, high initial U concentrations were decreased to below the MCL over the pH range 5.5−6.5 in the presence of newly formed CaUV solids, indicating that such solids can be important in controlling U in some environments.

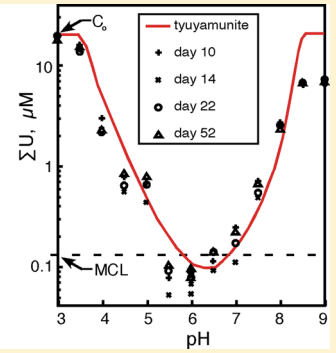

INTRODUCTION

Concentrations of uranium (U) in most groundwaters are commonly very low, rarely exceeding 80 nM.[1] However, groundwaters and surface waters associated with U mining and milling activities,[2−4] sites contaminated during the course of nuclear fuel and weapons production,[2,5−7] and environments surrounding U ore deposits[8−10] often have U concentrations considerably higher than the U.S. Environmental Protection Agency's maximum contaminant level (MCL) of 0.13 μM. When the total U concentration in sediments exposed to oxidizing waters in these environments is only slightly elevated, sorption may still be effective in moderating dissolved U(VI) concentrations, especially at neutral and near-neutral pH.[11] Under low pH, humic acids adsorbed on mineral surfaces have been found to strongly enhance UO_2^{2+} adsorption and removal from pore waters.[12] Nevertheless, finite sorption capacities will generally leave aqueous U concentrations above the MCL at higher total U concentrations. Aqueous uranyl−silica complexes can elevate dissolved U concentrations in the slightly acidic pH range.[13] At neutral to alkaline pH and higher CO_2 partial pressure, several aqueous uranyl carbonate complexes compete with U sorption and elevate dissolved U concentrations.[1,14] The $Ca_2UO_2(CO_3)_3$ aqueous complex[15,16] strongly competes with U(VI) sorption, especially when calcite is present.[17]

Under some reducing conditions, the U MCL can easily be met at higher total sediment U concentrations because of the lower solubility of amorphous U(IV) and crystalline uraninite (UO_2).[1] Thus, the need for remediating contaminated groundwaters has motivated a large number of studies on reduction, usually involving microbially driven U(VI) bioreduction stimulated through injection of organic carbon as the electron source.[3,18,19] However, stimulation of U bioreduction occurs at the cost of increased (bi)carbonate concentrations resulting from organic carbon oxidation, which promotes U dissolution through formation of aqueous uranyl carbonate complexes.[20−22] Furthermore, bioreduction-based U stabilization appears to require indefinite maintenance of the contaminated zone with a supply of reducing agent.[23]

In view of the prevailing oxidizing conditions in the vadose zone and shallow aquifers, understanding the solubility of U(VI) solids is important for predicting U behavior in environments containing high total U concentrations. Information on solubilities of U(VI) solids formed at low temperatures of soils and shallow groundwaters (rather than well-crystallized, lower solubility minerals formed at elevated temperatures and pressures) is particularly relevant for estimating long-term aqueous U concentrations in contaminated oxidizing, near-surface environments. Although most uranyl minerals are much more soluble than uraninite, U(VI) minerals are very diverse.[24] Therefore, examination of the

Received: March 9, 2012
Revised: June 19, 2012
Accepted: June 26, 2012
Published: June 26, 2012

solubility behavior of U(VI) solids under typical groundwater conditions is warranted in order to understand sediments containing elevated U, whether naturally or through contamination.

Like U, vanadium is redox sensitive, and commonly more soluble under oxidizing conditions.[25] Vanadium occurs in oxidation states III, IV, and V in near-surface environments. Monomeric vanadate, V(V), and oxoanions $H_2VO_4^-$ and HVO_4^{2-} prevail at typical groundwater concentrations (sub micromolar), although polymeric vanadates form at high (ca. millimolar) concentrations.[25,26] The reported pK_a values of these oxoanions vary considerably, with 8.75 recommended in the review by Larson.[26] Under highly acidic conditions (pH < 3.4), VO_2^+ forms rather than H_3VO_4.[26] Vanadate minerals that do not contain U include hewettite, $CaV_6O_{16}\cdot 9H_2O$, metahewettite, $CaV_6O_{16}\cdot 3H_2O$, and pascoite, $Ca_3(V_{10}O_{28})\cdot 17H_2O$, formed from oxidation of V-rich oxides and sulfides.[27,28] Complexation and reduction of aqueous V(V), and vanadyl, V(IV),[29] species lead to its accumulation in organic rich sediments.[30] Important V(III) minerals include montroseite, VO(OH),[31] and the mica clay roscoelite, $KAlV_2Si_3O_{10}(OH)_2$, in which V^{3+} substitutes for Al^{3+}.[32] These V minerals have been mined at numerous locations within the Colorado Plateau, Nevada, the Pasco region of Peru, Australia, Kazakhstan, and Gabon.

In environments where both U and V previously slowly accumulated through precipitation under reducing conditions and then reverted to oxidizing conditions, uranyl vanadate solids have commonly formed.[9,33−35] Among U(VI) minerals, some uranyl vanadates have very low solubilities; hence, they may control both U and V concentrations in environments where they occur.[9] The major uranyl vanadate minerals carnotite, $K_2(UO_2)_2V_2O_8\cdot 3H_2O$, metatyuyamunite, $Ca(UO_2)_2V_2O_8\cdot 3-5H_2O$, and tyuyamunite, $Ca(UO_2)_2V_2O_8\cdot 8H_2O$, have been reported in a variety of locations including the Colorado Plateau of the United States,[24,34,36] valleys and basins within Mexico,[33] Australia,[37] southern Africa,[38] the Pampean Ranges of Argentina,[39] and desert soils in Israel.[40] Indeed, with better understanding of uranyl vanadate solubilities, prospecting for U and V ores based on groundwater chemical analyses could be refined.[9,41] The very low estimated solubilities of these uranyl vanadate minerals suggest that they may even permit control of aqueous U concentrations below its MCL under some oxidizing conditions.

Although the occurrence and mineralogy of these U(VI) solids are known, their thermodynamic properties have only been estimated. Langmuir[34] calculated a $\Delta G_f^\circ = -4590$ kJ mol^{-1} for carnotite based on solubility data reported by Hostetler and Garrels[42] and calculated very low U concentrations in equilibrium with this mineral. At 1 mM K^+ and 1 μM V(V), U concentrations were predicted to be controlled below the MCL at circum-neutral pH. Our recent experiments on potassium uranyl vanadate precipitation at pH 6.0 and 7.8 (room temperature) were in fairly good agreement with calculations based on Langmuir's ΔG_f° value, despite the lack of detectable carnotite formation.[23] The amorphous solids precipitated in the recent study had K/U/V = 1.24:1.00:1.09, compared with 1:1:1 for carnotite.

To our knowledge, even less is known about the solubility of tyuyamunite. Langmuir combined his estimated ΔG_f° value for carnotite with an approximate ΔG_r° for the reaction between carnotite and tyuyamunite in order to estimate the ΔG_f° of tyuyamunite. The tyuyamunite−carnotite ΔG_r° was assumed to equal the ΔG_r° for the reaction between analogous Ca− and K−uranyl phosphates, autunite, and K−autunite.[34] We found no other publications on thermodynamic data for tyuyamunite or on experimental tests of aqueous U(VI) concentrations in equilibrium with tyuyamunite. However, improvements in understanding other factors relevant to tyuyamunite stability have emerged. These include further refinements to the aqueous speciation of U(VI),[43] in particular with respect to the $CaUO_2(CO_3)_3^{2-}$ and $Ca_2UO_2(CO_3)_3^0$ solution complexes,[15,16] and of V(V) speciation [26] made in recent years.

The objectives of this study are as follows: (i) model dissolved U concentrations in a generic groundwater in equilibrium with various U(VI) minerals in order to evaluate their potential for controlling U at its MCL; (ii) experimentally determine U(VI) concentrations in simple solutions containing Ca^{2+}, U(VI), and V(V); (iii) compare these experimental results with equilibrium predictions based on current thermodynamic data; and (iv) determine when tyuyamunite or other calcium uranyl vanadates could control U concentrations below its MCL.

MATERIALS AND METHODS

Equilibrium Calculations. Groundwater U speciation and concentrations were calculated for equilibrium with various U(VI) minerals using the Nuclear Energy Agency's updated U thermodynamic database,[43] along with additional ΔG_f° values listed in Table 1, using PHREEQC2.12.[44] The pH was varied from 4 to 8 in order to span most of the common groundwater range. A $pCO_2 = 2.5$ was used to represent departure from atmospheric equilibrium and to allow formation of uranyl carbonate aqueous complexes above levels reached at $pCO_2 = 3.5$. The total aqueous Ca^{2+} concentration was fixed at 1 mM to include formation of $Ca_2UO_2(CO_3)_3^0$ and $CaUO_2(CO_3)_3^{2-}$,[15,16] and the H_4SiO_4 concentration was about 1.8 mM (equilibrium with amorphous SiO_2) to include formation of $UO_2SiO(OH)_3^+$.[43] Other ions at fixed concentrations were Na^+ (7.9 mM), K^+ (0.1 mM), and NO_3^- (50 μM). For simplicity, Mg^{2+} was excluded from the calculations, although formation of $MgUO_2(CO_3)_3^{2-}$ needs to be considered in less common waters where concentrations of this cation greatly exceed those of Ca^{2+}.[16,45] Total dissolved phosphate was set to 1 μM, except for equilibria with autunite, in which case its concentration was determined by dissolution of the mineral. The pH-dependence total inorganic C was calculated for $pCO_2 = 2.5$, and the Cl^- concentration was varied for charge balance. Major minerals representative of different U(VI) groups were used individually as equilibrium phases. The selected pure minerals were schoepite, $[UO_3\cdot 2H_2O]$, becquerelite, $[Ca(UO_2)_6O_4(OH)_6\cdot 8H_2O]$, rutherfordine, $[UO_2CO_3]$, uranophane, $[Ca(UO_2)_2(SiO_3OH)_2\cdot 5H_2O]$, autunite, $[Ca(UO_2)_2(PO_4)_2\cdot 10-12H_2O]$, and tyuyamunite, $[Ca(UO_2)_2V_2O_8\cdot 8H_2O]$; chosen as representative uranyl oxyhydroxides, carbonates, silicates, phosphates, and vanadates, respectively.[24,43]

Precipitation Experiments. Laboratory batch solution experiments were conducted in order to determine U(VI) concentrations in the presence of Ca^{2+} and V(V) under oxidizing conditions. Uranyl nitrate hexahydrate (Spectrum Chemicals & Laboratory Products, ACS reagent), sodium metavanadate (Aldrich, 99.9% anhydrous), and calcium nitrate (Baker & Adamson, reagent) were used as starting reagents. Initially, acidic (pH ≈ 3) and alkaline (pH ≈ 9) stock solutions

Table 1. Thermodynamic Constants for Major Species (298.15 K) Used for Calculating U Concentrations[a]

species	ΔG_f°, kJ/mol	± kJ/mol	source
UO_2^{2+}	−952.6	±1.7	G
$UO_2CO_3^0$	−1537.2	±1.8	G
$UO_2(CO_3)_2^{2-}$	−2103.2	±2.0	G
$UO_2(CO_3)_3^{4-}$	−2660.9	±2.1	G
$(UO_2)_2CO_3(OH)_3^-$	−3139.5	±4.5	G
$CaUO_2(CO_3)_3^{2-}$	−3231.8	±7.1	DB
$Ca_2UO_2(CO_3)_3^0$	−3817.1	±6.2	DB
UO_2OH^+	−1159.7	±2.2	G
$UO_2(OH)_2$	−1357.5	±1.8	G
$UO_2(OH)_3^-$	−1548.4	±3.0	G
$UO_2(OH)_4^{2-}$	−1716.2	±4.3	G
$(UO_2)_2OH^{3+}$	−2126.8	±6.7	G
$(UO_2)_2(OH)_2^{2+}$	−2347.3	±3.5	G
UO_2Cl^+	−1084.7	±1.8	G
UO_2Cl_2	−1208.7	±2.9	G
$UO_2SiO(OH)_3^+$	−2249.8	±2.2	G
$UO_2PO_4^-$	−2053.6	±2.5	G
UO_2HPO_4	−2089.9	±2.8	G
$UO_2H_2PO_4^+$	−2108.3	±2.4	G
$UO_2(H_2PO_4)_2$	−3254.9	±3.7	G
$UO_2(H_2PO_4)(H_3PO_4)^+$	−3260.7	±3.7	G
H_2O	−237.14	±0.04	G
OH^-	−157.22	±0.07	G
HCO_3^-	−586.85	±0.25	G
CO_3^{2-}	−527.90	±0.39	G
$H_4Si(OH)_4$	−1307.74	±1.16	G
Cl^-	−131.22	±0.12	G
NO_3^-	−110.79	±0.42	G
$H_2PO_4^-$	−1137.15	±1.57	G
HPO_4^{2-}	−1095.98	±1.57	G
$H_2VO_4^-$	−1020.9	±0.5	Lar
HVO_4^{2-}	−974.5	±0.5	Lar
Ca^{2+}	−552.81	±1.05	G
K^+	−282.51	±0.11	G
Na^+	−261.95	±0.10	G
silica(amorphous), $SiO_2(am)$	−849.0		L
schoepite, $UO_3{\cdot}2H_2O$	−1632.5	±10.3	GH
rutherfordine, UO_3CO_3	−1564.7	±1.8	G
becquerelite-synthetic, $Ca(UO_2)_6O_4(OH)_6{\cdot}8H_2O$	−10311.1	±14.0	G
becquerelite-natural, $Ca(UO_2)_6O_4(OH)_6{\cdot}8H_2O$	−10371.1	±360	C, G
uranophane, $Ca(UO_2)_2(SiO_3OH)_2{\cdot}5H_2O$	−6196.1	±0.5	P
Ca−autunite, $Ca(UO_2)_2(PO_4)_2{\cdot}10H_2O$	−4763.9		L
tyuyamunite, $Ca(UO_2)_2V_2O_8{\bullet}8H_2O$	−4560.6		L

[a]Sources: (G) Guillaumont et al.,[43] (L) Langmuir,[1] (Lar) Larson,[26] (DB) from log K of Dong and Brooks,[16] combined with ΔG_f° values from Guillaumont et al., (GH) Giammar and Hering,[46] (C) Casas et al.,[47] (P) Prikryl[48].

of these salts were prepared with nitric acid (EMD chemicals, OmniTrace) and sodium bicarbonate (J.T.Baker, ACS reagent), respectively. Duplicate 40 mL batch solutions were prepared to contain components of the target calcium uranyl vanadate precipitate at initial concentrations of 20 μM U(VI), 20 μM V(V), and 60 μM Ca^{2+}, in 50 mL screw-cap Teflon vials. A higher relative amount of Ca^{2+} (in comparison to U and V) was used because of its typically higher concentration in groundwaters. The pH was adjusted to values ranging from 3.0 to 9.0, in 0.5 pH unit increments with either nitric acid or sodium hydroxide (J.T. Baker, ACS reagent). The middle pH condition of 6.0 was prepared from adjustments of both initially acidic and alkaline stock solutions, while all other samples were prepared only from the stock solution with pH closest to its target value. Other ions in solution were Na^+ (5−8 mM), NO_3^- (4−5 mM), and HCO_3^- (0−0.9 mM). The pH-adjusted (HNO_3 and NaOH) vials were placed on a shaker for continuous agitation, with periodic venting to equilibrate with atmospheric CO_2, and sampled at selected times for analysis of the aqueous phase chemical composition. Atmospheric CO_2 equilibrium was achieved, except in the pH 8.5 and 9 solutions. The presence of nitrate and regular opening of the vials for pH adjustment ensured that all solutions remained oxidizing. Prior to chemical analyses, solutions were centrifuged (3 h, 21 °C, 14 000g) to remove potentially suspended particles. Concentrations of U, V, and Ca were measured on days 1, 2, 6, 10, 14, 22, and 52 by inductively coupled plasma mass spectrometry (ICP-MS, ELAN DRC II, Perkin−Elmer).

Analyses of Precipitated Solid Phase. Larger, 250 mL batch solutions were prepared in order to precipitate sufficient quantities of solids for analyses. For this purpose, the Ca/U/V molar ratios in initial solutions were set to 1:2:2 of tyuyamunite. Initial solutions were prepared to contain 300 μM uranyl nitrate (hexahydrate), 300 μM sodium metavanadate, and 150 μM calcium chloride (dihydrate), and they were adjusted to pHs 4.5, 5.5, 6.0 6.5, and 7.5. Solutions were continuously agitated for at least 10 days, with periodic uncapping to equilibrate with atmospheric CO_2, followed by filtration through 80 nm polycarbonate filters in order to recover subsamples of the precipitated solids. The collected solids were split for two analyses: ICP-MS for determining ratios of Ca/U/V, and powder X-ray diffraction (XRD) or synchrotron μ-XRD (Advanced Light Source, beamline 12.3.2). The μ-XRD samples were sealed with Kapton tape, attached on a sample holder, and vertically mounted on the stage for transmission mode measurements. The μ-XRD measurements were obtained with monochromatic 10 keV X-rays and a MAR 133 CCD detector. Acquired spectra were analyzed with XMAS software (https://sites.google.com/a/lbl.gov/bl12-3-2/user-resources). An additional pH 6.0 precipitation test was conducted at 90 °C in order to enhance crystal formation for XRD analysis. This solution/suspension was kept in an oven, sealed in a Teflon bottle except for brief daily venting and stirring.

RESULTS AND DISCUSSION

Equilibrium Calculations. The calculations indicate that dissolution of most U(VI) minerals will lead to U concentrations that greatly exceed the MCL when equilibrated with groundwater (Figure 1). Rutherfordine is predicted to have U concentrations in excess of 1 mM over the full pH range and is therefore not shown in the figure. Calculated U concentrations in equilibrium with synthetic becquerelite, schoepite, and autunite are greater than 1 μM. Of the minerals considered in Figure 1, well-crystallized becquerelite, uranophane, and tyuyamunite appear capable of controlling U concentrations below the MCL in oxidizing environments, over a narrow circum-neutral pH range. With respect to becquerelite however, the higher solubility synthetic form is likely to be the potential U controlling mineral over relatively short time frames associated with contamination histories. Moreover, the magnitude of the reported solubility lowering for the well-

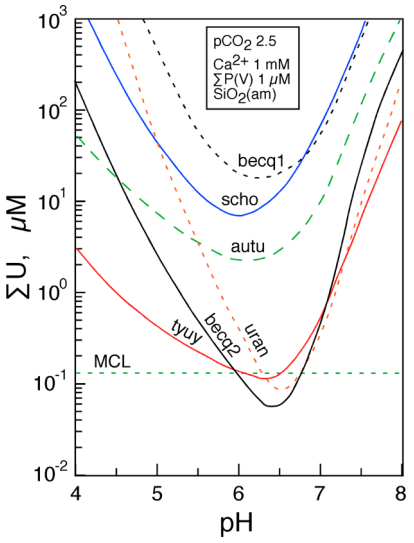

Figure 1. Calculated total dissolved U concentrations in oxidizing groundwaters, for equilibrium with different U(VI) minerals; schoepite [$UO_3 \cdot 2H_2O$], synthetic (becq1) and well-crystallized (becq2) becquerelite [$Ca(UO_2)_6O_4(OH)_6 \cdot 8H_2O$], uranophane [$Ca(UO_2)_2(SiO_3OH)_2 \cdot 5H_2O$], autunite [$Ca(UO_2)_2(PO_4)_2 \cdot 10\text{–}12H_2O$], and tyuyamunite [$Ca(UO_2)_2V_2O_8 \cdot 8H_2O$]. The pCO_2 = 2.5, Ca^{2+} = 1 mM, dissolved silica is in equilibrium with SiO_2(am), and the ionic strength = 10 mM.

crystallized becquerelite was considerably greater than expected for crystal size effects and therefore not recommended by Guillaumont et al.[43] A number of recent investigations have been conducted to improve understanding of the environmental behavior of uranophane group minerals.[5,48−51] As noted earlier, limited information is available on tyuyamunite solubility.

Several strong aqueous complexes of UO_2^{2+} are important at different pHs in dissolving U(VI) minerals exposed to typical groundwaters (Figure 2). At the lowest pH, uncomplexed UO_2^{2+} is dominant. Under slightly acidic to neutral pH, groundwaters typically contain dissolved silica at about millimolar concentrations, and the dominant uranyl solution species is expected to be the $UO_2SiO(OH)_3^+$ complex.[13] At neutral and higher pH, several U(VI)−carbonato complexes become important.[43] Given the common presence of Ca^{2+} at about 1 mM concentrations, $Ca_2UO_2(CO_3)_3$ and $CaUO_2(CO_3)_3^{2-}$ can be dominant U(VI) species at neutral to alkaline pH.[15,16] The very strong U(VI) aqueous complexes with silica and carbonate are evident in the calculated U(VI) speciation for equilibria with tyuyamunite shown in Figure 2. Given the common presence of dissolved silica and Ca^{2+} at concentrations of 1 mM and higher in groundwaters, even very low solubility U(VI) minerals appear to have fairly limited ability to control U below its MCL.

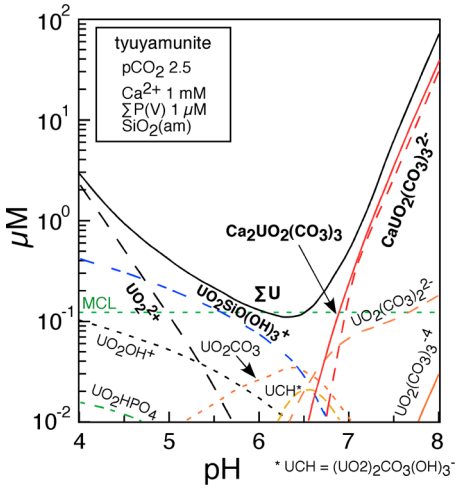

Figure 2. Calculated dominant aqueous uranyl species concentrations for equilibrium dissolution of tyuyamunite, at pCO_2 = 2.5, with Ca^{2+} = 1 mM, dissolved silica in equilibrium with SiO_2(am) (≈ 1.8 mM), and ionic strength = 10 mM.

Precipitation Experiments. Time trends in total dissolved U concentrations (∑U) in the pH-dependent precipitation experiment are presented in Figure 3, showing average values of duplicate samples (relative differences were <5%, except for a few early time conditions). Initially, rapid changes in U concentrations toward equilibrium levels were observed in the precipitation experiments. Large decreases in total dissolved U occurred within 4 h of pH adjustment for all but the most acidic (pHs 3.0 and 3.5) solutions. These initial decreases were followed by further declines in U concentration over the course of about 10 days and relatively steady concentrations over the remaining experimental time (Figure 3).

The total dissolved U(VI) and V(V) concentrations remaining in the batch solutions at later times (days 10−52) were fairly stable and are shown as functions of pH in Figure 4a and b, respectively. Data for ∑U from these later times are roughly similar to predictions for equilibrium with tyuyamunite, based on their solution chemistries and parameters listed in Table 1 (Figure 4a). The largest discrepancy between measured and modeled ∑U concentrations were found at pHs 8.5 and 9.0, where ∑U was high but significantly lower than predicted. Note that measured ∑U concentrations are below its MCL for 5.5 ≤ pH ≤ 6.5. Other model predictions for pH-dependent U concentrations shown in Figure 4a are for cases where solubilities are controlled by schoepite, synthetic becquerelite, and well-crystallized natural becquerelite. These model U concentrations will be briefly discussed in the context of anomalous behavior of V(V) measured in this experiment.

In contrast to the behavior of U, the stable V concentrations departed from levels predicted based on the estimated formation constant for tyuyamunite (Figure 4b). From pH 6.5 up to nearly pH 8.0, measured V concentrations in solutions remained about 1 order of magnitude greater than their predicted levels. The logarithmic concentration scales in Figure 4a, b makes visual evaluation of relative removal amounts of U versus V difficult. Ratios of V removed relative to U removed from these solutions (both components initially at 20 μM) are shown in Figure 4c. No precipitation occurred at pH 3.0, while the limited precipitation at pH 3.5 had a V/U molar ratio of about 2.3. From pH 4.0 up to 6.5, a nearly 1:1 molar removal occurred, consistent with precipitation of a tyuyamunite-like phase. At still higher pH, V/U removal ratios declined progressively, settling to about 0.5:1 at pH 9.0. This indicates that U was precipitated in other solid(s) with lower proportions of vanadate, although the other common nonvanadate U(VI) minerals are not predicted to control U at the low concentrations shown in Figure 4a, as illustrated by curves for schoepite and synthetic becquerelite. The well-crystallized natural becquerelite reported by Casas et al.[47] is predicted to leave U concentrations at far lower levels without removing V. Thus, precipitation of both tyuyamunite and well-crystallized

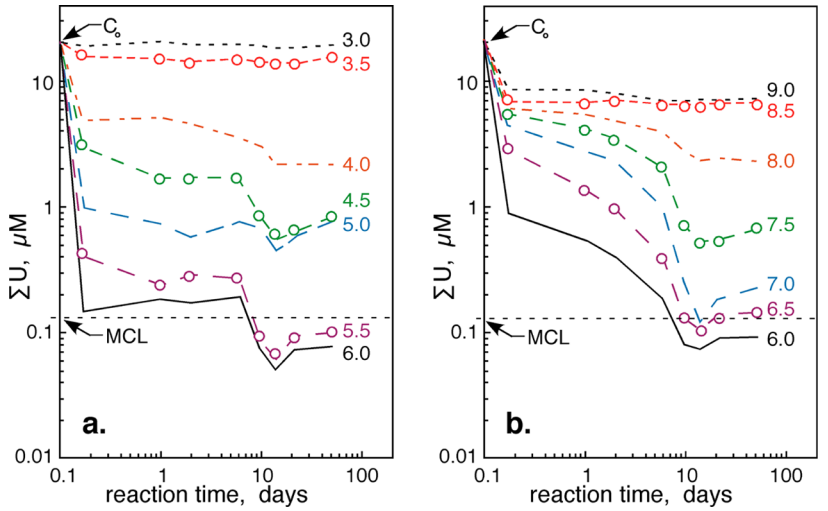

Figure 3. Time trends for total U(VI) concentrations in solutions equilibrating at different pH: (a) pH ≤6.0, and (b) pH ≥ 6.0. Initial concentrations are 60 μM Ca^{2+}, 20 μM $\sum$U(VI), and 20 μM $\sum$V(V), and $pCO_2 \approx 3.5$.

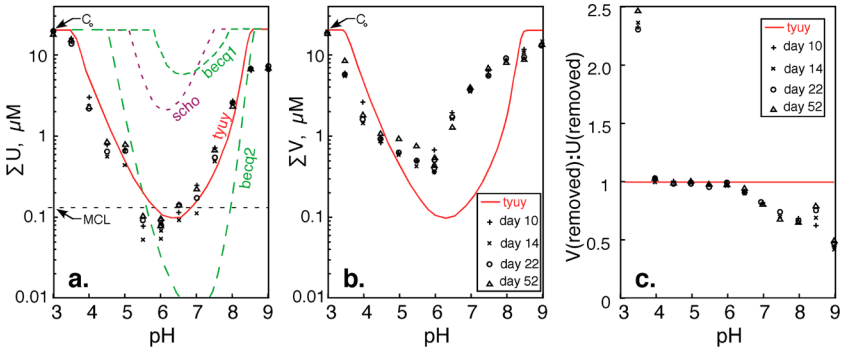

Figure 4. Comparisons between predicted equilibrium and measured longer term concentrations of (a) total aqueous U(VI), (b) total aqueous V(V), and (c) ratios of precipitated V to precipitated U. Initial concentrations are 60 μM Ca^{2+}, 20 μM $\sum$U(VI), and 20 μM $\sum$V(V), ionic strength ≈ 10 mM, and $pCO_2 \approx 3.5$. Calculated curves are for equilibrium with tyuyamunite (tyuy), schoepite (scho), laboratory-synthesized becquerelite (becq1), and well-crystallized natural becquerelite (becq2).

becquerelite might yield U and V concentrations shown in Figure 4a, b. However, such explanation appears implausible because formation of well-crystallized becquerelite in short-term room temperature experiments is unlikely and furthermore its stability constant is questionable.

Precipitated Solid Phase. The solid phase precipitated in larger volume batches was separated for analyses by ICP-MS, μXRD, and powder XRD. Elemental analyses (ICP-MS) of the precipitate formed in larger batch tests (room temperature) indicated that the solid phase Ca/U/V molar ratio ranged widely, from about 1:1:1 to 1:5:5, compared to the Ca/U/V in tyuyamunite of 1:2:2. The measured ratios of U/Ca, V/Ca, and V/U in the solids precipitated under the different pH conditions are shown in Figure 5 (data points), along with the corresponding ratios for tyuyamunite (dashed lines). Note that some of the U/Ca and V/Ca ratios were fairly close to the 1:2 of tyuyamunite when precipitated from acidic solutions (pH ≤ 6.0), but variations were still large (Figure 5a, b). Consistent with the solution phase analyses described previously, the measured V/U ratios in the precipitated solids (Figure 5c) were all fairly close to 1:1 associated with the uranyl vanadate sheet structure of tyuyamunite and carnotite.[52] The lack of distinct peaks in XRD patterns obtained from these solids precipitated at room temperature is consistent with the broad range of measured Ca/U/V molar ratios. Similar attempts to synthesize carnotite from room temperature aqueous solutions have not yielded a crystalline structure.[23,53] The powder XRD pattern obtained on the solid recovered from the 90 °C solution (equivalent room temperature pH = 6.0) was less noisy than the equivalent room temperature samples and did match two of the highest intensity peaks for tyuyamunite and metatyuyamunite (Supporting Information, Figures S1 and S2). Similar rough correspondence with these uranyl vanadates was found for a pH 5, room temperature sample (Supporting Information, Figure S3). Thus, the solids precipitated at lower temperature may eventually transform to tyuyamunite.

Implications. These experiments showed that U concentrations in the presence of sufficiently high levels of Ca^{2+} and V(V) will be controlled at levels close to those predicted with tyuyamunite being the solubility-determining mineral, despite the fact that the solid phases formed in our study were amorphous and lacked tyuyamunite's molar ratios of Ca, U, and V. The complex chemistries of both U and V apparently allow metastable amorphous solids to form under low temperature conditions of soils and groundwaters. Such solids may remain amorphous or poorly crystalline while moderating aqueous concentrations of both U and V. Equilibrium calculations predict that tyuyamunite and uranophane can control U at its MCL in some oxidizing environments, albeit over a narrow range of pH (ca. 6–7). Above neutral pH, the highly stable

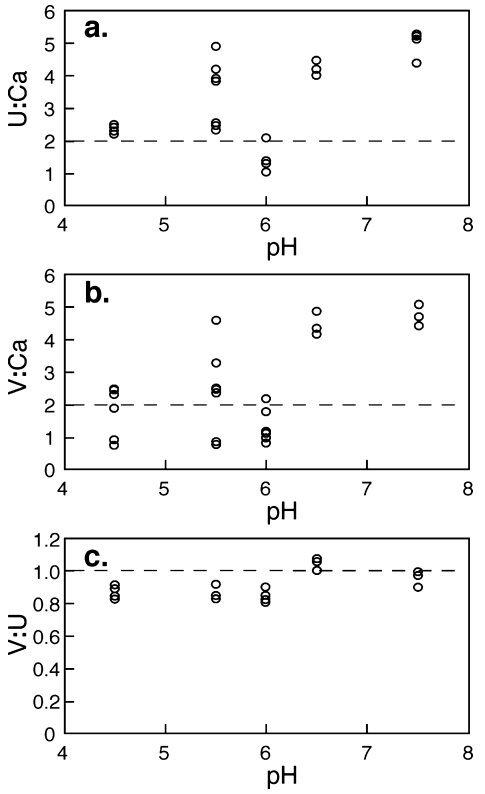

Figure 5. Element molar ratios in solids recovered from precipitation experiments (points), compared with values for tyuyamunite (dashed lines): (a) U/Ca ratios; (b) V/Ca ratios; and (c) V/U ratios.

carbonato−U and Ca−U−-carbonato complexes will keep aqueous U concentrations elevated even in the presence of tyuyamunite-like phases. Below pH 6, complexes with dissolved Si are predicted to elevate U concentrations. However, given variations in dissolved silica, (bi)carbonate, and Ca^{2+} concentrations in groundwaters, equilibrium with these U(VI) solids do not appear to suppress U concentrations at low enough levels to reliably meet regulatory goals.

■ ASSOCIATED CONTENT

Ⓢ Supporting Information

X-ray diffraction patterns from CaUV solid precipitated from pH 6 solution at 20 and 90 °C and from pH 5 solution at 20 °C.oom temperature and a 90 °C precipitated CaUV solids. This material is available free of charge via the Internet at http://pubs.acs.org.

■ AUTHOR INFORMATION

Corresponding Author

*Phone: (510) 486-7176; e-mail: tktokunaga@lbl.gov.

Notes

The authors declare no competing financial interest.

■ ACKNOWLEDGMENTS

Helpful comments from the reviewers are gratefully acknowledged. Funding was provided through the Subsurface Biogeochemical Research Program of the Office of Biological and Environmental Research, U.S. Department of Energy, under contract no. DE-AC02-05CH11231. We thank Martin Kunz for assistance with the μ-XRD measurements. The Advanced Light Source is supported by the Director, Office of Science, Office of Basic Energy Sciences, of the U.S. Department of Energy under contract no. DE-AC02-05CH11231.

■ REFERENCES

(1) Langmuir, D. *Aqueous Environmental Geochemistry*: Prentice-Hall: Upper Saddle River, NJ, 1997; p 600.

(2) Meinrath, A.; Schneider, P.; Meinrath, G. Uranium ores and depleted uranium in the environment, with reference to uranium in the biosphere from the Erzgebirge/Sachsen, Germany. *J. Environ. Radioact.* **2003**, *64*, 175−193.

(3) Anderson, R. T.; Vrionis, H. A.; Ortiz-Bernad, I.; Resch, C. T.; Long, P. E.; Dayvault, R.; Karp, K.; Marutzky, S.; Metzler, D. R.; Peacock, A.; White, D. C.; Lowe, M.; Lovley, D. R. Stimulating the in situ activity of Geobacter species to remove uranium from the groundwater of a uranium-contaminated aquifer. *Appl. Environ. Microbiol.* **2003**, *69*, 5884−5891.

(4) Landa, E. R. Uranium mill tailings: nuclear waste and natural laboratory for geochemical and radioecological investigations. *J. Environ. Radioact.* **2004**, *77*, 1−27.

(5) Catalano, J. G.; Heald, S. M.; Zachara, J. M.; Brown, G. E., Jr. Spectroscopic and diffraction study of uranium speciation in contaminated vadose zone sediments from the Hanford Site, Washington State. *Environ. Sci. Technol.* **2004**, *38* (10), 2822−2828.

(6) Serkiz, S. M.; Johnson, W. H.; Johnson-Wile, L. M.; Clark, S. B. Environmental availability of uranium in an acidic plume at the Savannah River Site. *Vadose Zone J.* **2007**, *6* (2), 354−362.

(7) Zachara, J. M.; Serne, J.; Freshley, M.; Mann, F.; Anderson, F.; Wood, M.; Jones, T.; Myers, D. Geochemical processes controlling migration of tank wastes in Hanford's vadose zone. *Vadose Zone J.* **2007**, *6* (4), 985−1003.

(8) Runnells, D. R.; Lindberg, R. D. Hydrogeochemical exploration for uranium ore deposits: Use of the computer model WATEQFC. *J. Geochem. Explor.* **1981**, *15*, 37−50.

(9) Langmuir, D.; Chatham, J. R. Groundwater prospecting for sandstone-type uranium deposits: A preliminary comparison of the merits of mineral-solution equilibria, ans single-element tracer methods. *J. Geochem. Explor.* **1980**, *13*, 201−219.

(10) Lehmann, B. Uranium ore deposits. *Rev. Econ. Geol. AMS Online* **2008**, *2008* (2), 16−26.

(11) Jenne, E. *Adsorption of Metals by Geomedia: Variables, Mechanisms, and Model Applications*; Academic Press: San Diego, CA, 1998; p 583.

(12) Wan, J. M.; Dong, W. M.; Tokunaga, T. K. Method to attenuate U(VI) mobility in acidic waste plumes using humic acids. *Environ. Sci. Technol.* **2011**, *45* (6), 2331−2337.

(13) Moll, H.; Geipel, G.; Brendler, V.; Bernhard, G.; Nitsche, H. Interaction of uranium(VI) with silicic acid in aqueous solutions studied by time-resolved laser-induced fluorescence spectroscopy (TRLFS). *J. Alloys Compd.* **1998**, *271*−*273*, 765−768.

(14) Stoliker, D. L.; Kent, D. B.; Zachara, J. M. Quantifying differences in the impact of variable chemistry on equilibrium uranium(VI) adsorption properties of aquifer sediments. *Environ. Sci. Technol.* **2011**, *45*, 8733−8740.

(15) Bernhard, G.; Geipel, G.; Reich, T.; Brendler, V.; Amayri, S.; Nitsche, H. Uranyl(VI) carbonate complex formation: Validation of the $Ca_2UO_2(CO_3)_3$ (aq.) species. *Radiochim. Acta* **2001**, *89*, 511−518.

(16) Dong, W.; Brooks, S. C. Determination of the formation constants of ternary complexes of uranyl and carbonate with alkaline earth metals (Mg^{2+}, Ca^{2+}, Sr^{2+}, and Ba^{2+}) using anion exchange method. *Environ. Sci. Technol.* **2006**, *40* (15), 4689−4695.

(17) Zheng, Z.; Tokunaga, T. K.; Wan, J. Influence of calcium carbonate on U(VI) sorption to soils. *Environ. Sci. Technol.* **2003**, *37* (24), 5603−5608.

(18) Lovley, D. R. Anaerobes to the rescue. *Science* **2001**, *293*, 1444−1446.

(19) Wall, J. D.; Krumholz, L. R. Uranium reduction. *Annu. Rev. Microbiol.* **2006**, *60*, 149−166.

(20) Wan, J.; Tokunaga, T. K.; Brodie, E. L.; Wang, Z.; Zheng, Z.; Herman, D. J.; Hazen, T. C.; Firestone, M. K.; Sutton, S. R. Reoxidation of bioreduced uranium under reducing conditions. *Environ. Sci. Technol.* **2005**, *39* (16), 6162−6169.
(21) Wan, J.; Tokunaga, T. K.; Kim, Y.; Brodie, E.; Daly, R.; Hazen, T. C.; Firestone, M. K. Effects of organic carbon supply rates on mobility of previously bioreduced uranium in a contaminated sediment. *Environ. Sci. Technol.* **2008**, *42*, 7573−7579.
(22) Tokunaga, T. K.; Wan, J.; Kim, Y.; Daly, R. A.; Brodie, E. L.; Hazen, T. C.; Herman, D.; Firestone, M. K. Influences of organic carbon supply rate on uranium bioreduction in initially oxidizing, contaminated sediment. *Environ. Sci. Technol.* **2008**, *42* (23), 8901−8907.
(23) Tokunaga, T. K.; Kim, Y.; Wan, J. Potential remediation approach for uranium-contaminated groundwaters through potassium uranyl vanadate precipitation. *Environ. Sci. Technol.* **2009**, *43* (14), 5467−5471.
(24) Finch, R.; Murakami, T. Systematics and paragenesis of uranium minerals. In *Uranium: Mineralogy, Geochemistry, and the Environment*; Burns, P. C., Finch, R., Eds.; Mineralogical Society of America: Washington, D.C., 1999; Vol. *38*, pp 91−179.
(25) Wanty, R. B.; Goldhaber, M. B. Thermodynamics and kinetics of reactions involving vanadium in natural systems: Accumulation of vanadium in sedimentary rocks. *Geochim. Cosmochim. Acta* **1992**, *56*, 1471−1483.
(26) Larson, J. W. Thermochemistry of vanadium(5+) in aqueous solutions. *J. Chem. Eng. Data* **1995**, *40* (6), 1276−1280.
(27) Evans, H. T. J. The crystal structure of hewettite. *Can. Mineral.* **1989**, *27*, 181−188.
(28) Swallow, A. G.; Ahmed, F. R.; Barnes, W. H. The crystal chemistry of pascoite, $Ca_3V_{10}O_{28}\cdot 17H_2O$. *Acta Crystallogr.* **1966**, *21*, 397−405.
(29) Wehrli, B.; Stumm, W. Vanadyl in natural waters: Adsorption and hydrolysis promote oxygenation. *Geochim. Cosmochim. Acta* **1989**, *53*, 69−77.
(30) Breit, G. N.; Wanty, R. B. Vanadium accumulation in carbonaceous rocks: A review of geochemical controls during deposition and diagenesis. *Chem. Geol.* **1991**, *91*, 83−97.
(31) Evans, H. T.; Garrels, R. M. Thermodynamic equilibria of vanadium in aqueous systems as applied to the interpretation of the Colorado Plateau ore deposits. *Geochim. Cosmochim. Acta* **1958**, *15*, 131−149.
(32) Meunier, J. D. The composition and origin of vanadium-rich clay minerals in Colorado Plateau Jurassic sandstones. *Clays Clay Miner.* **1994**, *42* (4), 391−401.
(33) Burciaga-Valencia, D. C.; Reyes-Cortes, M.; Reyes-Rojas, A.; Renteria-Villalobos, M.; Esparza-Ponce, H.; Fuentes-Cobas, L.; Fuentes-Montero, L.; Silva-Saenz, M.; Herrera-Peraza, E.; Munoz, A.; Montero-Cabrera, M. E. Characterization of uranium minerals from Chihuahua using synchrotron radiation. *Rev. Mex. Fis.* **2010**, *56* (1), 75−81.
(34) Langmuir, D. Uranium solution-mineral equilibria at low temperatures with applications to sedimentary ore deposits. *Geochim. Cosmochim. Acta* **1978**, *42*, 547−569.
(35) Frost, R. L.; Cejka, J.; Weier, M. L.; Martens, W.; Henry, D. A. Vibrational spectroscopy of selected natural uranyl vanadates. *Vib. Spectrosc.* **2005**, *39* (2), 131−138.
(36) Stern, T. W.; Stieff, L. R.; Girhard, M. N.; Meyrowitz, R. The occurrence and properties of metatyuyamunite, $Ca(UO_2)_2(VO_4)_2\cdot 3-5H_2O$. *Am. Mineral.* **1956**, *41* (3−4), 187−201.
(37) Arakel, A. V. Carnotite mineralization in inland drainage areas of Australia. *Ore Geol. Rev.* **1988**, *3*, 289−311.
(38) von Backstrom, J. W.; Jacob, R. E. Uranium in South Africa and South West Africa (Namibia). *Philos. Trans. R. Soc., A* **1979**, *291*, 307−319.
(39) Bertolino, S. R. A.; Zimmermann, U.; Sattler, F. J. Mineralogy and geochemistry of bottom sediments from water reservoirs in the vicinity of Cordoba, Argentina: Environmental and health constraints. *Appl. Clay Sci.* **2007**, *36*, 206−220.
(40) Ilani, S.; Strull, A. Uranium mineralization in the Judean Desert and in the Northern Negev, Israel. *Ore Geol. Rev.* **1989**, *4*, 305−314.
(41) Rose, A. W.; Wright, R. J. Geochemical exploration models for sedimentary uranium deposits. *J. Geochem. Explor.* **1980**, *13*, 153−179.
(42) Hostetler, P. B.; Garrels, R. M. Transportation and precipitation of uranium and vanadium at low temperatures, with special reference to sandstone-type uranium deposits. *Econ. Geol.* **1962**, *57* (2), 137−167.
(43) Guillaumont, R.; Fanghanel, T.; Fuger, J.; Grenthe, I.; Neck, V.; Palmer, D. A.; Rand, M. H.; Mompean, F. J.; Illemassene, M.; Domenechi-Orti, C. *Update on the Chemical Thermodynamics of Uranium, Neptunium, Plutonium, Americium, and Technicium*; Elsevier: Amsterdam, The Netherlands, 2003.
(44) Parkhurst, D. L.; Appelo, C. A. J. User's Guide to PHREEQC (Version 2)−A Computer Program for Speciation, Batch-Reaction, One-Dimensional Transport, and Inverse Geochemical Calculations. http://wwwbrr.cr.usgs.gov/projects/GWC_coupled/phreeqc/, 2005.
(45) Dong, W.; Brooks, S. C. Formation of aqueous $MgUO_2(CO_3)_3^{2-}$ complex and uranium anion exchange mechanism onto an exchange resin. *Environ. Sci. Technol.* **2008**, *42* (6), 1979−1983.
(46) Giammar, D. E.; Hering, J. G. Influence of dissolved sodium and cesium on uranyl oxide hydrate solubility. *Environ. Sci. Technol.* **2004**, *38* (1), 171−179.
(47) Casas, I.; Bruno, J.; Cera, E.; Finch, R. J.; Ewing, R. C. Characterization and dissolution behavior of a becquerelite from Shinkolobwe, Zaire. *Geochim. Cosmochim. Acta* **1997**, *61* (18), 3879−3884.
(48) Prikryl, J. D. Uranophane dissolution and growth in $CaCl_2$−SiO_2(aq) test solutions. *Geochim. Cosmochim. Acta* **2008**, *72* (18), 4508−4520.
(49) Arai, Y.; Marcus, M. A.; Tamura, N.; Davis, J. A.; Zachara, J. M. Spectroscopic evidence for uranium bearing precipitates in vadose zone sediments at the Hanford 300-area site. *Environ. Sci. Technol.* **2007**, *41* (13), 4633−4639.
(50) Shvareva, T. Y.; Mazeina, L.; Gorman-Lewis, D.; Burns, P. C.; Szymanowski, J. E. S.; Fein, J. B.; Navrotsky, A. Thermodynamic characterization of boltwoodite and uranophane: Enthalpy of formation and aqueous solubility. *Geochim. Cosmochim. Acta* **2011**, *75*, 5269−5282.
(51) Um, W.; Wang, Z.; Serne, R. J.; William, B. D.; Brown, C. F.; Dodge, C. J.; Francis, A. J. Uranium phases in contaminated sediments below Hanford's U tank farm. *Environ. Sci. Technol.* **2009**, *43* (12), 4280−4286.
(52) Appleman, D. E.; Evans, H. T. The crystal structures of synthetic anhydrous carnotite, $K_2(UO_2)_2V_2O_8$, and its cesium analogue, $Cs_2(UO_2)_2V_2O_8$. *Am. Mineral.* **1965**, *50* (7,8), 825−842.
(53) Barton, P. B. Synthesis and properties of carnotite and its alkali analogues. *Am. Mineral.* **1958**, *43* (9,10), 799−817.

DISCLAIMER